Journal of Sciences, Islamic Republic of Iran 32(1): 53 - 61 (2021) http://jsciences.ut.ac.ir
University of Tehran, ISSN 1016-1104

DFT Study of Methanol Adsorption on Vacancy and N-Doped Graphene and Comparing Them with Pristine Graphene

F. Naderi[1], M. Menatian[2*], R. Behjatmanesh-Ardakani[2], H. Reza Zare-Mehrjardi[2]

[1] *Department of Chemistry, Shahr-e Qods Branch, Islamic Azad University, Tehran, Islamic Republic of Iran*
[2] *Department of Chemistry, Payame Noor University, P.O. Box:19395-3697 Tehran, Islamic Republic of Iran*

Received: 7 June 2020 / Revised: 14 September 2020 / Accepted: 25 November 2020

Abstract

In this study, density functional theory was used to investigate the effect of adsorption process and interaction between methanol as a fuel and graphene as a catalyst. Thermodynamic studies in this field have shown that Gibb's free energy is positive in most cases. Therefore, adsorption of methanol on graphene is very low and in the physical mode. Thus, other ways are required to increase adsorption on graphene surface. Changing pristine graphene (PG) to vacancy graphene (VG) or N-doped graphene (NG) can increase absorption, and convert their adsorption into chemical adsorption. Vacancy and N-doped in electronic structure of graphene increase adsorption of methanol to graphene. Increased absorption of VG and NG, in addition to changes in charge transfer causes significant changes in the location of HOMO and LUMO, which was confirmed by adsorption energy, NBO, QTAIM, and DOS.

Keywords: Adsorption Energy; Density Functional Theory; Methanol; N-Doped Graphene; Vacancy Graphene.

Introduction

Air pollution and greenhouse gases are the most important problems in the developed countries; the main source of which is emission of exhaust gases from motor vehicles. As the number of vehicles increases, greenhouse gas emission also increases, and global oil reserves decrease every day, as a result of which the use of alternative fuels will increase shortly. Methanol (CH_3OH) is used as a liquid alternative fuel [1]. Transportation, storage, distribution, and the use of methanol are similar to traditional gasoline fuel. For this reason, it is the most suitable and practical fuel for engines [2, 3]. Ignition temperature of alcohol is higher than that of gasoline, making it easier to transport and store. Exhaust gases produced from combustion of gasoline have a higher concentration of particulate matter and nitrogen oxides than those produced from combustion of methanol. There is an oxygen atom in structure of methanol molecule, making mixture of gasoline and methanol to have more oxygen. There have been several studies on the use of methanol-gasoline

* Corresponding author: Tel: +989186140862; Fax: +988433382132; Email: am.menatian@gmail.com

mixtures as fuel in spark ignition (SI) engines. *CO* and *NOx* emissions are reduced by increasing methanol in methanol/ gasoline mixture, while it is accompanied by fuel savings of 5.7–15% [4, 5). Thus, the combined use of fumigation methanol and oxidation catalyst leads to a decrease in the concentrations of *HC, CO, and NOx,* as well as particulate mass and number of the engine [6]. Graphene, a layer of graphite is the thinnest *2D* material. Graphene index properties can be used in many technologies [7, 8]. Also, electrical properties of graphene can be altered by doping nitrogen atoms or creating vacancy. Graphene bed catalyst with nitrogen dope provides excellent activity and durability for methanol oxidation reaction [9, 10]. According to the previous density functional theory (DFT) studies on graphene, it has been found that defects in graphene or doping of elements, such as N, Pt, Pd, Ru, Al, Fe, and Mn to graphene increase graphene uptake [11-15]. Investigation of electrical properties of *(N-doped and vacancy)* graphene bonding structures is important in terms of state density [16, 17. Both methods *(N-doped and vacancy)* can change electrical demand for graphene. In VG, vacancy increases concentration of a zigzag edge of carbon atoms in the graphene, which in turn reduces gap energy and increases adsorption energy. Usually, in doping, hetero atoms replace carbon atom in the graphene carbon lattice, such as nitrogen atom, which greatly expands applications of graphene [18.

In this study, DFT of adsorption energy of methanol on graphene is investigated with various configurations. Their effects on electronic structure of the modified surfaces are also evaluated. To the best of our knowledge, such studies have not been performed at this level before [19, 20. What seems important in this study is pivotal role of the combined use of CH_3OH in fuel, development of progressive methods, and introduction of new adsorbents. In theory, properties of CH_3OH interaction on surface of the above graphene are studied. Geometry, electronic structure, energy calculations, load analysis, and graphene energy gap mentioned in methanol adsorption are also assessed. For this purpose, basic information about the adsorbed methanol on graphene is determined, such as optimal orientation of interaction (adsorption) energy at various coverages and distances from graphene. Then, these data will be available as input for fine-tuning of molecular dynamics simulations of methanol adsorption process.

Materials and Methods

Optimization quantum chemistry and frequency calculations of all the geometric structures were performed using *Gaussian 09* software package by DFT at the *M062X* method with *6-31 G (d)* basis set, for obtaining real functions [21-24]. In this study, adsorption of *MeOH* onto surfaces of pristine graphene (PG), N-doped graphene *(NG), and* vacancy graphene *(VG)* was considered as adsorbent. There are three possible places for methanol to be adsorbed by graphene including top (methanol just on a carbon atom), bridge (methanol on a carbon-carbon bond), and hollow (methanol at the center of a graphene ring). Hydrogen atoms cap ends of these cells to neutralize electronic charge of terminal carbons. Methanol interacts with carbon, where changes, such as voids or nitrogen doping occur. The effects of these changes were also compared. Distance of methanol on graphene is the same for all the graphene settings and at a distance of fewer than 2**Å**. For comparing electrical changes of *PG, VG,* and *NG,* electronic structure descriptors must be calculated. Adsorption energy (*Eads)* and density of states *(DOS)* have been determined using the above theory level through energy of the highest occupied molecular orbital *(HOMO)* and energy of the lowest unoccupied molecular orbital *(LUMO)* from DFT, global electrophilicity index *(ω),* energy gap *(ΔEg),* chemical potential *(μ),* chemical hardness *(η),* softness *(S),* the highest amount of electronic charge *(ΔNmax),* Gibbs free energy *(Gibbs)*, corrections ,and basis set superposition error (*BSSE*) [25].

Adsorption energy *(Eads)* of CH_3OH on graphene was specified using *Eq. (1):*

$$\Delta E_{ads} = E_{(adsorbent- CH3OH)} - (E_{adsorbent} + E_{CH3OH}) + BSSE \quad (1)$$

Where, $E_{(adsorbent- CH3OH)}$ is the total energy of *adsorbent – CH_3OH system*, $E_{adsorbent}$, and E_{CH3OH} are the total adsorbent energies of the isolated material and methanol, respectively. Energies were corrected by considering zero-point energy *(ZPE)* and *BSSE* using the Boys-Bernardi reciprocal method.

After adsorption of *CH3OH* on different graphene configurations, charge transfer between them was investigated. Mechanism of interaction is as follows by comparing *HOMO* and *LUMO* between methanol and adsorbent after *CH3OH* adsorption:

$$\Delta Eg = - (E_{HOMO} - E_{LUMO}) \quad (2)$$

Where, E_{HOMO} and E_{LUMO} are the energies of *HOMO* and *LUMO, respectively*.

Chemical potential *(μ)* is defined based on the subsequent equation [26].

$$\mu = (E_{LUMO} + E_{HOMO})/2 \quad (3)$$

Also, chemical hardness *(η)* can be calculated through the *Koop-mans'* theorem (27).

$$\eta = (E_{LUMO} - E_{HOMO})/2 \quad (4)$$

In *1999, Parr et al.*, explained electrophilicity *(ω)*

concept and softness for the first time ,which is calculated as follows [28].

$$\omega=\frac{\mu^2}{2\eta} \quad (5)$$

Hardness measures charge flow that differs in electronegativity commends. Softness*(S)* is the inverse of hardness [29]. Eq. (6).

$$S=\frac{1}{2}\eta \quad (6)$$

The highest amount of electronic charge, ΔN_{max}, accepted by the electronic system is given by Eq. (7).

$$\Delta N_{Max}=-\mu/\eta=(\mu_B-\mu_A)/(\eta_A+\eta_B) \quad (7)$$

Natural bond orbitals (*NBO*) and natural atomic orbital occupancies were obtained by NBO analysis. At the same level, and with graphical figures of *NBO* generated by the Jmol *NBO* program, a graphical representation of *NBO*s was used [30-32].

$$\varepsilon=\frac{\lambda 1(r)}{\lambda 2(r)}-1 \quad (8)$$

$Where, \lambda 1$ and $\lambda 2$ are the first and second lowest eigenvalues of the Hessian matrix of ρ (r), respectively. At bond critical point, $\lambda 1$ and $\lambda 2$ are both negative and exhibit curvature of electron density perpendicular to bond path. Parameter ε *(r)* is a measure to determine nature of (*p*) and (*r*) bonds .An increase in the bond ellipticity indicates that nature of critical point deviates from (*r*) to (*p*). The more negative the *Hamiltonian* at critical point of the bond, the more covalent the bond [33, 34].

Results and Discussion

Adsorption Energy

Interaction of methanol as fuel and different configurations of graphene *(Pristine/ N-doped/ Vacancy)* as a catalyst was analyzed in different configurations. Figure 1 shows the optimized structure of *PG-CH₃OH* in the top and side views.

The optimized geometric shapes of graphene in different configurations are as follows: pristine graphene *(PG),* N-doped graphene *(NG),* and vacancy graphene *(VG)* were considered as adsorbent. Figure 2 presents the optimized geometric shape of different

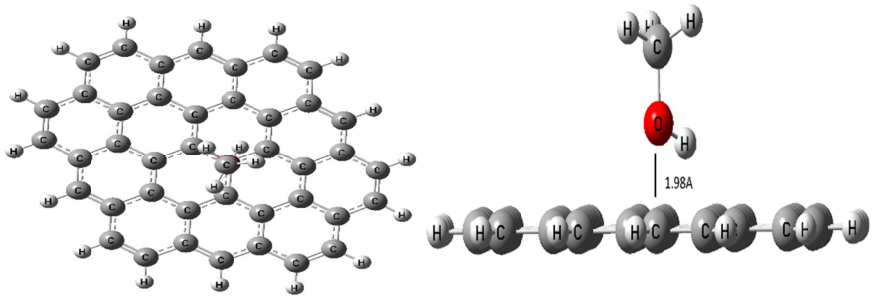

PG-CH_3OH (top view) PG-CH_3OH (side view)

Figure1. The optimized geometries of methanol on pristine graphene in the top and side views

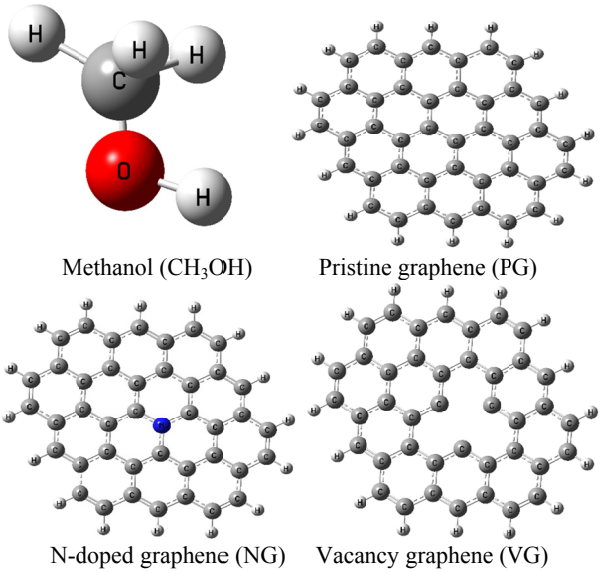

Methanol (CH_3OH) Pristine graphene (PG)

N-doped graphene (NG) Vacancy graphene (VG)

Figuer 2. The optimized geometric shape of (Pristine / N-doped / Vacancy) graphene and methanol molecule

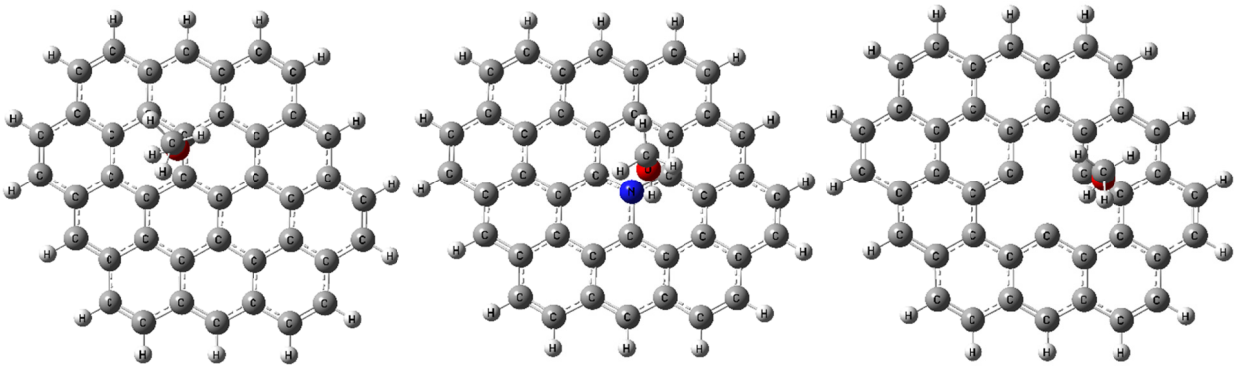

A) PG-CH_3OH B) NG-CH_3OH C) VG-CH_3OH

Figure 3. The optimized geometries of methanol on graphene in different configurations

configurations of graphene and methanol.

For this purpose, graphene was designed in different configurations to adsorb methanol by the *Gauss View 06* project. Quantum chemistry calculations of all the geometrical configurations were optimized using the *Gaussian 09* software package by the *M062X* method and basis set *6-31G (d),* which were as follows: PG-CH3OH, NG-CH3OH, and VG-CH3OH in bridge position (Fig. 3).

Table 1 shows the calculated values for adsorption energy *(E_{ads}),* obtained by *M062X /6–31G(d),* frontier molecular orbital and orbital characteristic including E_{HOMO}, E_{LUMO}, Gibbs energy *(Gibbs)*, energy gap *(Eg)* and corrections as well as *BSSE and* adsorption energy *(E_{ads})*.

In all the configurations, bridge positions were more energetically favorable than top or hollow positions (according to Table 1). Energy in bridge position was similar to intermediate energy in top and hollow positions. *VG-CH_3OH* was more energetically favorable than *NG-CH_3OH* and *PG-CH_3OH*. However, in the present study, it was found that the effect of vacancy

Table 1. Reactivity descriptors of all the investigated complexes in gas phase at *M062X /6–31 G (d)* level of theory. In different (top/bridge/hollow) positions, the letter t denotes to top, h denotes to hollow, and b denotes to bridge.

System	EHOMO (ev)	ELUMO (ev)	Eg (ev)	Gibbs (Ha)	BSSE (kcal/mol)	Eads (kcal/mol)
CH3OH	-9.244	3.392	-	-115.62	-	-
PG	-5.607	-1.735	-	-1609.35	-	-
NG	-5.807	-1.840	-	-1625.94	-	-
VG	-5.558	-1.844	-	-1570.99	-	-
PG-CH3OH(t)	-5.7647	-1.6966	4.0681	-1724.97	0.0036	2.259
PG-CH3OH(h)	-5.8736	-1.8098	4.0637	-1724.97	0.0032	2.008
PG-CH3OH(b)	-5.7541	-1.6876	4.0665	-1724.97	0.0037	2.322
NG-CH3OH (t)	-5.7464	-1.6425	4.1021	-1741.56	0.0023	1.443
NG-CH3OH (h)	-5.8883	-1.9560	3.9323	-1741.56	0.0023	1.443
NG-CH3OH (b)	-5.7604	-1.7875	3.9729	-1741.56	0.0022	1.380
VG-CH3OH(t)	-6.0989	-2.5113	3.5876	-1686.63	0.0041	-9.977
VG-CH3OH (h)	-5.9563	-2.2591	3.6972	-1686.63	0.0041	-9.977
VG-CH3OH (b)	-6.0643	-2.3742	3.6901	-1686.63	0.0035	-10.354

was greater than that of N-doped. Although, adsorption energy for both was greater than that of pristine graphene, adsorption energy *(VG-CH_3OH)* with ΔE_{ads} = *-10.354 kcal/mol* was more than all the graphene configurations. Also, it had the lowest adsorption energy of *(PG-CH_3OH)* with ΔE_{ads} = *2.322 kcal/mol*. The increase in nitrogen atoms doped to graphene influences the energy adsorbed by methanol to graphene. In the present study, the following method was confirmed by the data presented in Table 1 for adsorption energy of methanol on graphene.

VG-CH3OH (-10.354kcal/mol) > NG-CH3OH (1.380kcal/mol) > PG-CH3OH (2.322kcal/mol)

Density of State (DOS)

For investigating adsorption of methanol molecules on graphene surface, density of state *(DOS)* and *HOMO-LUMO* band gap in all the complexes were plotted using *Gauss-Sum3* software and were compared with pristine graphene (Fig. 4). *DOS* graphs can be used as an important tool to analyze nature of the interaction.

Figure. 4 presents HOMO and LUMO molecular orbitals for all the graphene modes from top and side views. The positive effect of vacancy and *N*-doped was revealed by comparing *DOS* of all the graphene states. Little difference was also found in hybridization between them. Comparison of the effect of vacancy and N-doped on graphene with pristine graphene in methanol adsorption systems showed that these effects increase *HOMO* and decrease *LUMO* energies. Ultimately, it reduces energy gap since there is an inverse relationship between gap energy and adsorption energy [35, 36]. These effects reduce gap energy and increase adsorption energy (Table 1).

VG- CH_3OH (Eg=3.69ev) < NG-CH_3OH (Eg=3.97ev) <PG-CH_3OH (Eg=4.07ev)

In the top and side views, molecular orbitals of *HOMO* and *LUMO* for different configuration positions of methanol and graphene are shown (Fig. 5). In *PG*, *HOMO* circuit covers *C-C* bonds, while *LUMO* circuits cover interacting carbon atoms. After *vacancy* or *N-doped* graphene, both *HOMO* and *LUMO* orbitals fall into carbon atoms around vacancy and *N* atom, resulting in higher *VG* and *NG* adsorption than *PG*.

Compared to *PG*, *HOMO* and *LUMO* molecular orbitals in *NG* mainly surround *N* atom and give

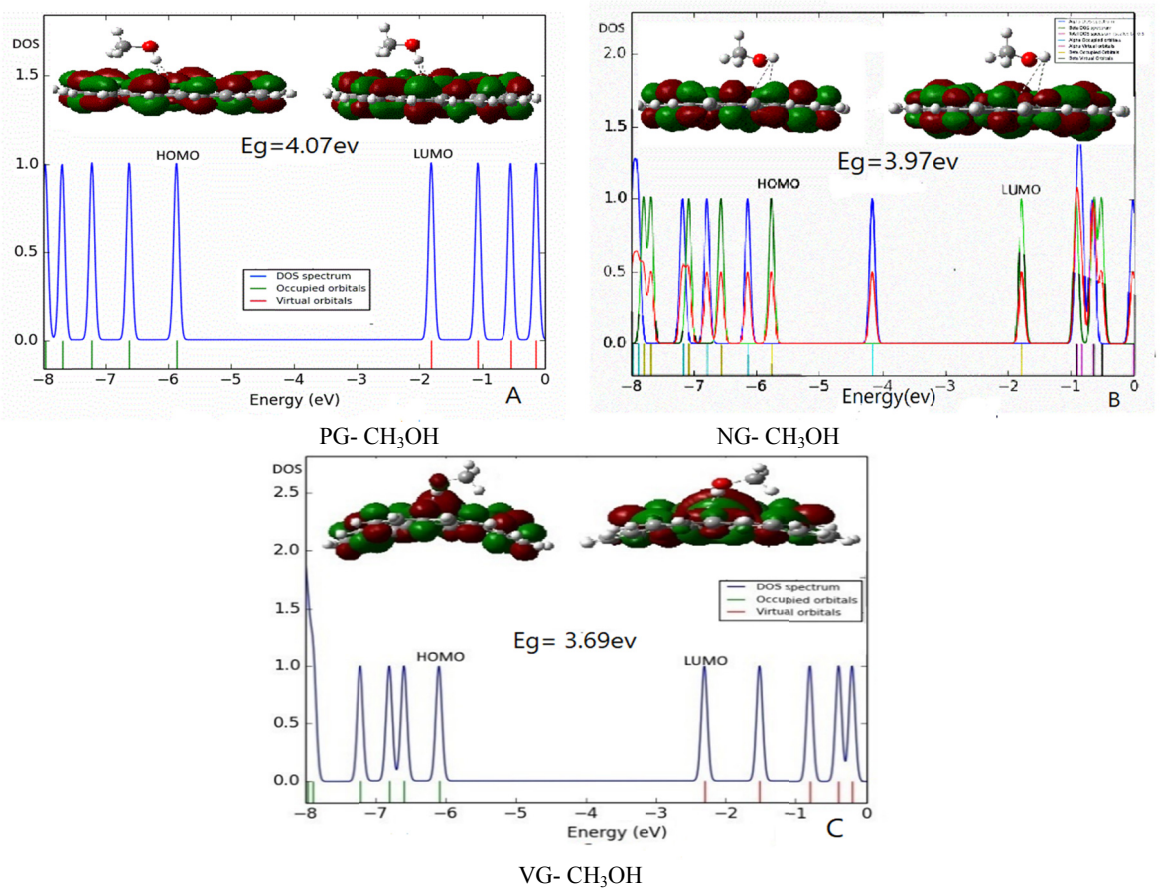

PG- CH_3OH NG- CH_3OH

VG- CH_3OH

Figure 4. DOS graphs with HOMO and LUMO orbitals for methanol adsorption on graphene

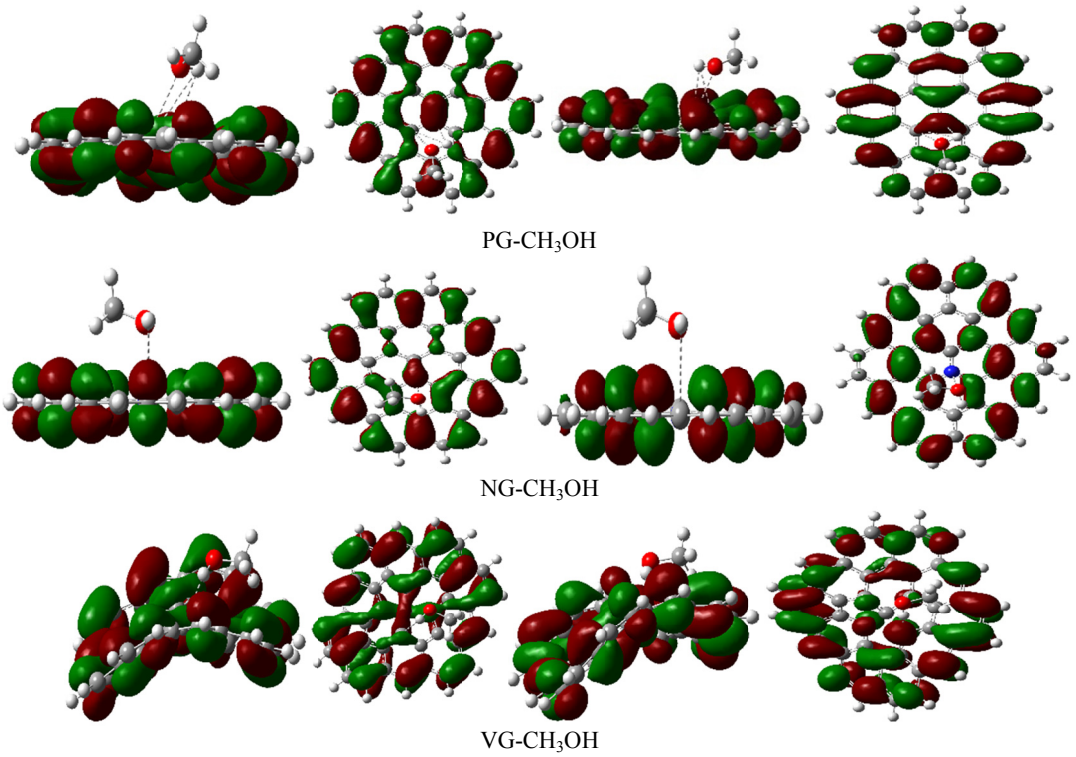

Figure 5. HOMO and LUMO molecular orbitals for different configurations of methanol and graphene in top and side views

unparalleled properties to bonds and atoms around nitrogen, reducing energy gap *(Eg)* by about *0.6* volts (Table 1). Thus, it can be concluded that this decrease in *Eg* increases *NG* absorption relative to *PG* (Fig. 5).

But both *HOMO* and *LUMO* orbitals cover oxygen atom by absorbing *CH_3OH* to *NG*, leading to an increase in *Eg* (Table 2), meaning that *NG-CH_3OH* complex is more stable than *NG*. In comparison of *VG* with *PG*, vacancy increases concentration of a zigzag edge of carbon atoms in the graphene, which in turn reduces gap energy and increases adsorption energy [37]. As shown in Table 2, hardness of the system increases by absorbing *CH_3OH* to graphene. Based on the principle of maximum stiffness defined by *Ralph G Pearson* [38], a system with more hardness is more stable. This means that stability is increased by absorbing *CH_3OH* in *VG*. Also, electricity of resulting complex is significantly reduced compared to *VG*, indicating an increase in its stability. Charging transmission may also be described in terms of

Table 2. Electron parameter before and after methanol adsorption in various graphene states, and in different (top/bridge/hollow) positions.

System	$Q_{mulliken}$ (ev)	Q_{NPO} (ev)	μD (debye)	μ	η	S	ω	ΔN_{Max}
CH3OH	-0.642	-0.634	0.106	2.925	6.319	3.159	0.677	0.463
PG	-0.237	-0.251	0.135	3.671	1.936	0.969	3.480	1.896
PG-CH3OH(t)	-0.633	-0.756	0.137	-3.731	2.034	1.017	3.422	1.834
PG-CH3OH(h)	-0.644	-0.750	0.141	3.842-	2.032	1.016	2.632	1.891
PG-CH3OH(b)	-0.633	-0.756	0.137	3.721-	2.033	1.016	3.405	1.830
NG	-1.084	-0.333	0.141	3.823-	1.984	0.992	3.683	1.927
NG-CH3OH (t)	-1.084	-0.751	0.136	3.693-	2.051	1.025	3.325	1.801
NG-CH3OH (h)	-1.086	-0.750	0.144	3.922-	1.966	0.983	3.912	1.995
NG-CH3OH (b)	-1.078	-0.763	0.139	3.774-	1.986	0.993	3.586	1.900
VG	-0.233	-0.257	0.136	3.700-	1.857	0.928	3.686	1.993
VG-CH3OH(t)	-0.672	-0.784	0.140	-4.305	1.794	0.897	5.165	2.400
VG-CH3OH (h)	-0.636	-0.765	0.132	-4.108	1.849	0.925	4.563	2.222
VG-CH3OH (b)	-0.648	-0.764	0.136	4.219-	1.845	0.923	4.824	2.287

electronic chemical potential and chemical hardness through Pearson equations, as well as in global electrophysical concept introduced by *Parr et al*. [39, 40].

NBO Analysis

In quantum chemistry, an NBO is a calculated bonding orbital with maximum electron density. Natural orbitals are used in computational chemistry to calculate distribution of electron density in atoms and bonds between the atoms [41]. Table 3 shows net charge transfer from CH3OH adsorption to graphene surface using NBO. *Lewis acid* is a chemical compound that contains an empty orbital, capable of accepting a lone pair from the *Lewis base. Lewis base* is a compound containing a lone pair that may form a covalent bond with *Lewis acid*. *NBO* is used to confirm pure charge transfer between methanol layers of *PG, NG,* and *VG.* Electrical charge distribution in *NG* indicated that *N* atom adsorbs electrons of surrounding carbon atoms and increases density of the electrons surrounding nitrogen. Also, electrical charge distribution in *VG* indicated that electron density of carbon atoms around cavity is increased compared to other carbon atoms, which increases their adsorption reaction. In *PG,* charge of all carbon atoms is neutral because their adsorption is a kind of *Lewis acid/ base*. Therefore, there is no tendency in graphene to adsorb methanol oxygen. As a result, adsorption energy of methanol to virgin graphene is minimal (see Table 3). In comparison of adsorption of *PG* with *NG,* it was found that electric charge of atoms is equal to *-0.020 and -0.331* in *PG* and *NG, respectively.* Because graphene is an electron donor and methanol is an electron receptor, *N*-doped into graphene increases negative charge in *NG* over *PG. NG* increases absorption relative to *PG.* In comparison of *PG* absorption with *VG,* it was revealed that electric charge is *equal to -0.020 and -0.090* in *PG* and *VG, respectively.* The increase in the negative charge in *VG* was not large enough to influence this. Therefore, it can be said that another factor has increased absorption of *VG.* Unsaturated carbon atoms in *VG* increase adsorption, but when *N* is doped to *VG,* it becomes saturated, which reduces adsorption of graphene, but also increases negative electric charge in nitrogen atom, which in turn increases absorption in graphene. However, the effect of unsaturation is greater than negative charge on atoms, so *VG* has the highest adsorption among graphene in different configurations. As shown in Figure.6 and Table 3, the following trend is confirmed by adsorption of methanol to graphene.

QTAIM Analysis

The theory of atoms in a molecule was introduced by Richard Bader. This theory defines chemical structure of a system based on distribution of electron density between two atoms. Figure 7 demonstrates molecular graphs, where the positions of all bond critical points *(BCPs)* between methanol and graphene are indicated.

The existence of *BCPs* is evidence for formation of chemical bonds between interacting atoms.

Tables 4 and 5 present the calculated values of electron density *ρ(r),* Laplacian $(\nabla^2\rho)$, and other characteristics ,such as bond ellipticity *(ε),* potential energy density *(V),* kinetic energy density *(G),* the total energy density *(H)* , the ratio of $\frac{|V(r)|}{G(r)}$and eigenvalues of Hessian matrix, and Hessian matrix eigenvalues .

Positive and large $(\nabla^2\rho)$ and ***ρ(r),*** values can make a chemical bond stronger than the others. Charge density

Table 3. The results obtained regarding load *(NBO)* and bond between atoms.

System	bond	Bond length (Å)	QNBO of atom 1	QNBO of atom 2
PG- CH_3OH	C_{17}–C_{26}	1.40	C_{17}=-0.003	C_{26}=-0.008
NG- CH_3OH	C_{27}-N_{64}	1.41	C_{27}=+0.235	N_{64}=-0.331
VG- CH_3OH	C_{25}-C_{26}	1.41	C_{25}+0.083	C_{26}=-0.096

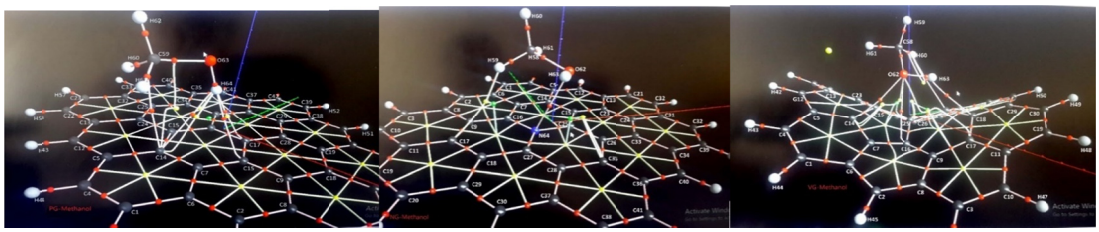

PG-CH_3OH *NG-CH_3OH* *VG- CH_3OH*

Figure 7. The obtained *QTAIM* molecular graphs of the studied complexes

Table 4. QTAIM topological parameters for the studied complexes

Complex	CP	BD	ε	G(r)	H(r)	V(r)	$\frac{\lvert V(r)\rvert}{G(r)}$
PG-CH3OH	(3,-1)	H64-C14	10.333	0.0061	-0.0014	0.0046	0.754
PG-CH3OH	(3,-1)	C59-C5	0.625	0.0052	-0.0011	0.0040	0.784
NG-CH3OH	(3,-1)	N64-O62	0.9696	0.0090	-0.0006	0.0084	0.933
NG-CH3OH	(3,-1)	N64-C27	0.0673	0.2474	0.4282	0.6757	2.731
VG-CH3OH	(3,-1)	O62-C14	3.4545	0.0073	-0.0010	0.0063	0.863
VG-CH3OH	(3,-1)	O62-C16	1.4782	0.0076	-0.0009	0.0067	0.882

Table 5. QTAIM topological parameters at BCPs of the studied complexes (all in a.u.)

Complex	CP	BD(Å)	$\rho(e/a_0^3)$	$\nabla^2\rho(e/a_0^5)$	λ1	λ2	λ3
PG-CH3OH	(3,-1)	H64-C14	0.0072	-0.0076	-0.0034	-0.0003	0.0341
PG-CH3OH	(3,-1)	C59-C5	0.0074	-0.0064	-0.0026	-0.0016	0.0299
NG-CH3OH	(3,-1)	N64-O62	0.0105	-0.0096	-0.0065	-0.0033	0.0483
NG-CH3OH	(3,-1)	N64-C27	0.2869	0.1809	-0.5502	-0.5155	0.3423
VG-CH3OH	(3,-1)	O62-C14	0.0090	-0.0084	-0.0049	-0.0011	0.0396
VG-CH3OH	(3,-1)	O62-C16	0.0095	-0.0085	-0.0057	-0.0023	0.0422

ρ(r) is low. Nature of interactions is of the weak ***Van der Waals*** forces and if signs of ***ρ(r)*** and ***H*** oppose each other, the bond is partially covalent and partially electrostatic.

The $\frac{|V(r)|}{G(r)}$ ratio is a suitable parameter to classify interatomic interactions. Electrostatic interactions are associated with $\frac{|V(r)|}{G(r)} \leq$ ***1***,intermediate interactions ***1*** $< \frac{|V(r)|}{G(r)} >$ ***2***, and the shared interactions $\frac{|V(r)|}{G(r)} >$ ***2*** (42). According to Table (4), where, $\frac{|V(r)|}{G(r)}$ is less than one in most cases and both Laplace and Hamilton values are positive or very low and electron densities are low, so the interaction is more likely to be of ***Van der Waals*** type. This is a weak attraction, but the effects of vacancy or doped increase electron density, which adds to adsorption property and transmits adsorption from ***Van der Waals*** force to electro-valence force. This confirms an increase in the adsorption energy.

Conclusions

In the present study, DFT calculations were performed to characterize adsorption ability of methanol onto pristine, ***vacancy***, and ***N-doped*** graphene, and their results were compared. As expected and according to the previous DFT studies, our results showed that the effect of vacancy and N-doped on graphene increases absorption. However, vacancy was more efficient than N-doped, so VG had the highest and PG had the lowest adsorption among graphene in different configurations. Poor adsorption of this molecule by PG and strong adsorption by VG and NG were confirmed by adsorption energy (Eads), and analyses, such as NBO, QTAIM, and DOS. The following method was confirmed by data about methanol energy absorption on graphene.

VG-CH_3OH> NG-CH_3OH> PG-CH_3OH

The interaction between methanol and graphene is of ***Van der Waals*** type. This force is a weak attraction and is considered as physical adsorption because values of ***Laplacian*** and ***Hamilton*** are positive or very low and electron density is low, but *vacancy* and *N-doped* effects increase electron density, which converts the force between methanol and graphene from ***Van der Waals*** to ***electro Valence***, which is a chemical adsorption and increases adsorption energy.

References

1. Schröder E. Methanol Adsorption on Graphene. *J Nanomater*. 2013;13:1303-3774.
2. Elfasakhany A. Performance and emissions of spark-ignition engine using ethanol–methanol–gasoline, n-butanol–iso-butanol–gasoline and iso-butanol–ethanol–gasoline blends: a comparative study. Int J Eng Sci Technol. 2016;19(4):2053-9.
3. Bata RM, Roan VP. Effects of Ethanol and/or Methanol in Alcohol-Gasoline Blends on Exhaust Emissions. J Eng Gas Turbines Power. 1989;111(3):432-8.
4. BahattinÇelik M, Özdalyan B, Alkan F. The use of pure methanol as fuel at high compression ratio in a single cylinder gasoline engine. Fuel. 2011;90(4):1591-8.
5. Wang X, Ge Y, Liu L, Peng Z, Hao L, Yin H, et al. Evaluation on toxic reduction and fuel economy of a gasoline direct injection- (GDI-) powered passenger car fueled with methanol–gasoline blends with various substitution ratios. Appl Energy. 2015;157:134-43.
6. Zhang Z, Cheung C, Chan T, Yao C. Emission reduction from diesel engine using fumigation methanol and diesel oxidation catalyst. Science of the Total Environment. 2009;407(15):4497-505.
7. Stankovich S, Dikin DA, Dommett GH, Kohlhaas KM, Zimney EJ, Stach EA, et al. Graphene-based composite materials. nature. 2006;442(7100):282-6.

8. Huang X, Qi X, Boey F, Zhang H. Graphene-based composites. Chem Soc Rev. 2012;41(2):666-86.
9. Xu X, Zhou Y, Yuan T, Li Y. Methanol electrocatalytic oxidation on Pt nanoparticles on nitrogen doped graphene prepared by the hydrothermal reaction of graphene oxide with urea. Electrochim Acta. 2013;112:587-95.
10. Zhang L-S, Liang X-Q, Song W-G, Wu Z-Y. Identification of the nitrogen species on N-doped graphene layers and Pt/NG composite catalyst for direct methanol fuel cell. Phys Chem Chem Phys. 2010;12(38):12055-9.
11. Jia X, Zhang H, Zhang Z, An L. Effect of doping and vacancy defects on the adsorption of CO on graphene. Materials Chemistry and Physics. 2020;249:123114.
12. Zhu X, Zhang L, Zhang M, Ma C. Effect of N-doping on NO2 adsorption and reduction over activated carbon: An experimental and computational study. Fuel (Guildford). 2019;258:116109.
13. Dong L, Gari RRS, Li Z, Craig MM, Hou S. Graphene-supported platinum and platinum–ruthenium nanoparticles with high electrocatalytic activity for methanol and ethanol oxidation. Carbon. 2010;48(3):781-7.
14. Rad AS. Density functional theory study of the adsorption of MeOH and EtOH on the surface of Pt-decorated graphene. Physica E: Low-dimensional Systems and Nanostructures. 2016;83:135-40.
15. Kiyani R, Rowshanzamir S, Parnian MJ. Nitrogen doped graphene supported palladium-cobalt as a promising catalyst for methanol oxidation reaction: Synthesis, characterization and electrocatalytic performance. Energy. 2016;113:1162-73.
16. Lv R, Terrones M. Towards new graphene materials: Doped graphene sheets and nanoribbons. Mater Lett. 2012;78:209-18.
17. Zhao XW, Tian YL, Yue WW, Chen MN, Hu GC, Ren JF, et al. Adsorption of methanol molecule on graphene: Experimental results and first-principles calculations. Int J Mod Phys B. 2018;32(09):1850102.
18. Wang H, Maiyalagan T, Wang X. Review on Recent Progress in Nitrogen-Doped Graphene: Synthesis, Characterization, and Its Potential Applications. ACS Catalysis. 2012;2(5):781-94.
19. Doronin M, Bertin M, Michaut X, Philippe L, Fillion J-H. Adsorption energies and prefactor determination for CH3OH adsorption on graphite. J Chem Phys. 2015;143:084703.
20. Xu X, Zhou Y, Lu J, Tian X, Zhu H, Liu J. Single-step synthesis of PtRu/N-doped graphene for methanol electrocatalytic oxidation. Electrochim Acta. 2014;120:439-51.
21. Becke AD. Density-functional thermochemistry. III. The role of exact exchange. J Chem Phys. 1993;98(7):5648-52.
22. Calais J-L. Density-functional theory of atoms and molecules. R.G. Parr and W. Yang, Oxford University Press, New York, Oxford, 1989. IX + 333 pp. Price £45.00. Int J Quantum Chem. 1993;47(1):101-.
23. Lee C, Yang W, Parr RG. Development of the Colle-Salvetti correlation-energy formula into a functional of the electron density. Phys Rev B. 1988;37(2):785-9.
24. Frisch MJ, Trucks GW, Schlegel HB, Scuseria GE, et.al. G09. Exp limit comput chem 2009.
25. ShokuhiRad A, Shabestari SS, Jafari SA, Zardoost MR, Mirabi A. N-doped graphene as a nanostructure adsorbent for carbon monoxide: DFT calculations. Molecular Physics. 2016;114(11):1756-62.
26. Chattaraj PK, Sarkar U, Roy DR. Electrophilicity Index. Chem Rev. 2006;106(6):2065-91.
27. Morrison RC. The extended Koopmans' theorem and its exactness. The Journal of Chemical Physics. 1992;96(5):10.1063/1.461875.
28. Parr RG, Szentpály Lv, Liu S. Electrophilicity Index. Journal of the American Chemical Society. 1999;121(9):1922-4.
29. Liu G-H, Parr RG. On Atomic and Orbital Electronegativities and Hardnesses. J Am Chem Soc. 1995;117(11):3179-88.
30. Raju HB, Goldberg JL. Nanotechnology for ocular therapeutics and tissue repair. Expert Review of Ophthalmology. 2008;3(4):431-6.
31. Shao Y, Wang J, Wu H, Liu J, Aksay IA, Lin Y. Graphene Based Electrochemical Sensors and Biosensors: A Review. Electroanalysis. 2010;22(10):1027-36.
32. Marcou G, Flamme B, Beck G, Chagnes A, Mokshyna O, Horvath D, et al. In silico Design, Virtual Screening and Synthesis of Novel Electrolytic Solvents. Molecular Informatics. 2019;38(10):1900014.
33. Rozas I, Alkorta I, Elguero J. Behavior of Ylides Containing N, O, and C Atoms as Hydrogen Bond Acceptors. J Am Chem Soc. 2000;122(45):11154-61.
34. Politzer P, Murray JS. Quantitative Analyses of Molecular Surface Electrostatic Potentials in Relation to Hydrogen Bonding and Co-Crystallization. Cryst Growth Des. 2015;15(8):3767-74.
35. Esfandfard SM, Elahifard M, Behjatmanesh-Ardakanii R, Kargar H. DFT study on oxygen-vacancy stability in rutile/anatase TiO2: Effect of cationic substitutions. Physical Chemistry Research. 2018;6:547-63.
36. Khosravi A, Vessally E, Oftadeh M, Behjatmanesh-Ardakani R. Ammonia capture by MN4 (M = Fe and Ni) clusters embedded in graphene. Journal of Coordination Chemistry. 2018;71(21):3476-86.
37. O'Boyle N, Tenderholt A, Langner K. cclib: A Library for Package-Independent Computational Chemistry Algorithms. J Comput Chem. 2008;29(5):839-45.
38. Bader RFW. Atoms in Molecules: A Quantum Theory (International Series of Monographs on Chemistry (22)). Science & Math. 1994;22:458.
39. Padmanabhan J, Parthasarathi R, Elango M, Subramanian V, Krishnamoorthy BS, Gutierrez-Oliva S, et al. Multiphilic Descriptor for Chemical Reactivity and Selectivity. J Phys Chem A. 2007;111(37):9130-8.
40. Islam DN, Ghosh D. On the Electrophilic Character of Molecules Through Its Relation with Electronegativity and Chemical Hardness. Int J Mol Sci. 2012;13:2160-75.
41. Weinhold F, Landis CR. NATURAL BOND ORBITALS AND EXTENSIONS OF LOCALIZED BONDING CONCEPTS. Chemistry Education Research and Practice. 2001;2(2):91-104.
42. Ziolkowski M, Grabowski SJ, Leszczynski J. Cooperativity in hydrogen-bonded interactions: ab initio and "atoms in molecules" analyses. J Phys Chem A. 2006;110(20):6514-21.